RSC Advances

This is an *Accepted Manuscript*, which has been through the Royal Society of Chemistry peer review process and has been accepted for publication.

Accepted Manuscripts are published online shortly after acceptance, before technical editing, formatting and proof reading. Using this free service, authors can make their results available to the community, in citable form, before we publish the edited article. This *Accepted Manuscript* will be replaced by the edited, formatted and paginated article as soon as this is available.

You can find more information about *Accepted Manuscripts* in the **Information for Authors**.

Journal Name

ARTICLE TYPE

Protein engineering of a new recombinant peptide to increase the surface contact angle of the stainless steel

X.Y. Ren[a,d], X.Q. Bai[a], C.Q. Yuan[a]*, Y.Yang[b], H. Xie[c], P. Cao[a] , C.Y. Ma[a] , X.J. Wang[a] and X.P. Yan[a]

Biofouling seriously affects the properties and the service life of metal materials. A number of studies have been shown that the initial bacterial attachment to the metal surface and the subsequent formation of biofilm are dependent on the surface characteristics of the substratum, including metal surface free energy, roughness and metallurgical features. In this study, a novel recombinant fusion protein which consisted of receptor binding domain protein (RBD), truncated protein fragment of MrpF and alkaline phosphatase (PhoA) domains has been constructed attempting for increasing the surface contact angle of stainless steel. It has been confirmed that RBD had a strong affinity to 304 stainless steel, whilst truncated protein fragment of MrpF had high hydrophobicity and anchoring features, which can improve the contact angle of material surface, whilst PhoA was an effective detecting tool to monitor the expression and secretion of fusion protein. Multiple assays including FTIR, XPS, SEM-EDS and contact angle measurement revealed the existing of nitrogen and sulfur elements, binding energy shift of nitrogen, carbon and oxygen atoms, the new FTIR peaks in treated stainless steel samples with increased contact angle about 50ºC, confirming that the new organic steel material has been produced responding to these surface property changes. Using novel recombinant peptides to react with steel could become a new technique to increase the surface contact angle of the stainless steel for diverse applications.

Keywords: Metal affinity; Stainless steel; Contact angle; Recombinant fusion protein

1. Introduction

The sections under the marine waterlines which immerse in seawater for a long time are frequently adhered by adhesive bacteria and/or bacillariophyta etc. This process leads to the formation of biofilm. Then the biofilm attracts a large number of fouling organisms, resulting in adhered fouling on the surface of the metal[1]. According to incomplete statistics, the damage causing by the biofouling can reach tens of billions dollars a year due to the increase of ship drag, for example[2].

However, the biofouling starts from the formation of the biofilm. If the early evolvement process of biofilm is prevented, the adhesion of subsequent macrofauna will be prevented. Therefore, increasing attention has been recently paid to alter the surface properties of material surface via surface modification[3,4].

The initial bacterial attachment to the metal surface and the subsequent formation of biofilm are dependent on the surface characteristics of the substratum, including surface free energy, roughness, as well as metallurgical features[5]. Thus, to gain low surface energy and adhesive force by surface modification has become a widespread acceptable strategy. Many pure natural extract with antifouling biological properties have been investigated, and the extract contains organic acid, inorganic acid, lactones, terpenoids, protein, polypeptide, sugar, fat and alkaloid etc[6].

Most recently, it has been found that a receptor binding domain (RBD) displaying at the type IV pili (T4P) of *Pseudomonas aeruginosa* (PA), consisting of a semi conserved 17-amino acid region that includes an intra-chain disulfide loop, has an extremely high affinity for stainless steel. The RBD can alter physical/chemical attributes of the untreated 304 stainless steel. The reaction products of RBD with regular 304 stainless steel significantly reduced the adhesive force and increased electron work function, and higher hardness of the steel[7].

MrpF is a part of Mrp operon in basophilic bacteria. Its gene length is about 282bp, coding the protein with 94 amino acids. By the computer prediction, it has been found that MrpF is simple in structure. It contains three transmembrane helix and has the characteristic of hydrophobic. In the previous research, truncated protein fragment of MrpF still has the properties of hydrophobicity and anchoring[8]. The fusion protein can anchor to

the cell membrane by the truncated protein fragment of MrpF, and interestingly this anchoring force is relatively weak so that extraction of the fusion protein is relatively ease[9]. Hence, the cells are not necessary to be broken to extract the fusion protein
5 and the extracting protein solution will have less impurities.

Alkaline phosphatase (PhoA) is a very common genetic engineering tool enzyme and has been widely used in pharmaceutical production, cosmetics manufacturing, disease detection etc[10]. The PhoA from *E.coli* is a secreted proteins that
10 usually are founded in the periplasmic space of *E. coli*. One end of the PhoA sequence has signal peptide. The membrane transport proteins can identify this signal peptide to secrete the PhoA into periplasmic space. In this process, the signal peptide is usually cleaved and only the PhoA which arrived periplasmic
15 space has biological activity[11]. Therefore, by inserting PhoA sequence to targeted fusion protein and detecting alkaline phosphatase activity can preliminarily monitor the expression and secretion of the targeted fusion protein.

In this study, we are specifically interested at design and
20 production of a novel fusion protein from the truncated MrpF fragment, RBD of pseudomonas aeruginosa type IV pili (T4P) and the PhoA of *E.coli* by genetic recombination. We hypothesize that the new fusion protein will do not only has the high affinity to metal, but also the strong hydrophobicity. The
25 protein reacting with stainless steel via a previously unreported type of chemical interaction will generate an altered form of stainless steel which is defined as bioorganic stainless steel. Thus the contact angle of the new bioorganic stainless steel could be lower than the untreated 304 stainless steel.

30 ## 2. Materials and methods

2.1 Vector design

To construct the plasmids vector for RBD-MrpF recombinant protein production, template plasmid pYC[PhoA-MrpF(L11)] (pYC) was used following the previous reported method[9]
35 (Fig.1A). The generation of the plasmid pXY[RBD-PhoA-MrpF(L11)] (RPM) (Fig.1B) was achieved by reverse PCR using primers PPSR and PPSF (Table 1). In plasmid pXY[RBD-PhoA-MrpF(L11)], the RBD gene was inserted into pMAL-p4x between PhoA signal peptide and phoA. Another plasmid
40 pXY[PhoA-RBD-MrpF(L11)] (PRM) (Fig.1C) was achieved by reverse PCR using primers PPFR and PPFF (Table 1). In the plasmid PRM, the RBD gene was inserted into pMAL-p4x between PhoA and MrpF instead of the Sac I.
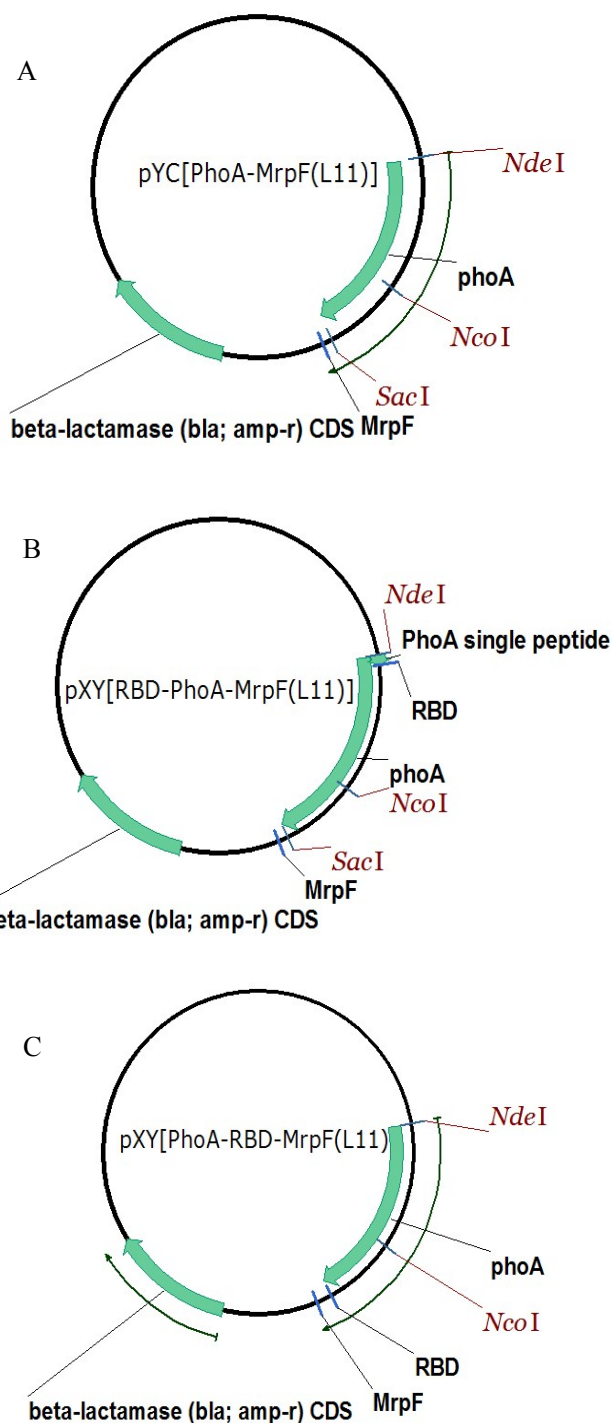
Fig.1 Schematic maps of plasmids for constructing of the vectors of recombinant protein. A) Plasmid pYC[PhoA-MrpF(L11)], the template plasmid. B) Plasmid pXY[RBD-PhoA-MrpF(L11)], in
50 which the RBD gene was inserted into pMAL-p4x between PhoA signal peptide and the rest of PhoA sequence. C) Plasmid pXY[PhoA-RBD-MrpF(L11)], in which the RBD gene was inserted into pMAL-p4x between PhoA and MrpF instead the Sac I.

In these plasmids, MrpF was the truncated protein fragment of MrpF. It still has the properties of hydrophobicity and anchoring. Because of its anchoring effect, the fusion protein can be anchored on the cell membrane. However its sequence is shorter
5 than full length of MrpF, its anchoring effect is weak and the fusion proteins can be peeled off from the membrane by weaker shocks. PhoA was used as a detection tool. PhoA is a secreted protein that usually is founded in the periplasmic space. If the PhoA is secreted into periplasmic space, it has the enzyme
10 activity. Therefore, detecting alkaline phosphatase activity is used to preliminarily monitor the expression and secretion of the target fusion protein.

To confirm the structure of the new vector, screening PCR was conducted by using primers PAF and mal R1 for RPM and
15 primers PhoA F2 and PAR for PRM (Table 1). DNA sequencing was performed by the Sangon Biotech (shanghai) Co., Ltd. The construct was transformed into *E. coli* strain BL21 (DE3) (from laboratory of living material of Wuhan university of technology) to express recombinant proteins. Primer PhoA F2 was the
20 sequencing primer for PRM and primer Mal promoter F was the sequencing primer for RPM. Table 1 lists all PCR primers used in this study.

2.2 Cell growth and expression of recombinant protein

25 A single colony of *E. coli* BL21 (DE3) harboring expression vectors was inoculated into Luria-Bertani medium containing 100μg/ml ampicillin and shaken at 37ºC overnight. The cell suspension was inoculated into M9 medium at a ratio of 1:50, cultured by shaking at 37ºC until an optical density (OD) at
30 600nm (OD600) reached 0.4-0.8. Protein expression was initiated by adding 1 mM growth repressor, isopropyl-β-D-thiogalactoside (IPTG), and continuing shaking at 25ºC. After 3 h induction, cell

suspension was sampled to assay the enzyme activity and the remaining cell suspension was harvested by centrifugation at
35 5000g for 10 min.

2.3 Extraction of recombinant protein and its analysis

The recombinant proteins were extracted by osmotic shock. Osmotic shock was based on a previously reported method[12]. Cells were re-suspended in buffer A (20% sucrose, 50 mM Tris-
40 HCl, pH 8.0), followed by shaking at room temperature for 10 min, then centrifuged at 8000g for 5 min. The pellet was re-suspended in ice water and shaken in an ice bath for 10 min. The suspension was centrifuged at 12000g for 10 min at 4ºC. The supernatant was collected for further analysis and use. In order to
45 maximize the extraction yield, the precipitation was carried out through a twice osmotic shock cycle. Two extracted protein solutions were pooled for further protein quantification and reaction with 304 stainless steel.

In order to preliminarily assess whether the fusion protein was
50 expressed, its enzyme activity was examined. The PhoA activity assay for cells treated by chloroform and SDS was based on a previously reported method[13]. Cells were washed with PBS and re-suspended in buffer B (1 M Tris-HCl, pH 8.0, 0.1 mM $ZnCl_2$). The equal volumes of chloroform and 0.1% SDS were added into
55 cell suspension, and incubated at 37ºC for 5 min to permeate cells. Then, the cell suspension was diluted by buffer B and adjusted OD600 between 0.1 and 0.2. After 0.4% p-nitrophenyl phosphate was added, cell suspension were incubated at 37ºC for 10 min. OD405 and OD550 were monitored after that. PhoA activity was
60 calculated using formula (1):

$$activity = \frac{(OD405 - 1.75 \times OD550) \times 1000}{time(\min) \times OD600 \times vol.celles(ml)} \qquad (1)$$

65
Table 1 Primers used in this study

Primers	Sequence 5'-3'	Applications
PPSF	gataacaaatatctgccgaaaacctgccagacccggacaccagaaatgcctg	Reverse PCR primer for RPM
PPSR	cggcagatatttgttatccgcgttgctggtgcacgcggcttttgtcacagggg	Reverse PCR primer for RPM
PPFF	gataacaaatatctgccgaaaacctgccagaccaacaacaacaacaataac	Reverse PCR primer for PRM
PPFR	cggcagatatttgttatccgcgttgctggtgcacgctttcagccccagagcggc	Reverse PCR primer for PRM
PhoA F2	gaccgaaagcaacgtacc	Screening and sequencing primer for PRM
PAR	tctggcaggttttcggcag	Screening primer for PRM
PAF	accagcaacgcggataac	Screening primer for RPM
mal R1	aggggatgtgctgcaag	Screening primer for RPM
Mal promoter F	acttcaccaacaaggacc	Sequencing primer for RPM

To determine whether the extracted protein solution contained the fusion protein and whether the fusion protein had biological activity, enzyme activity detection of the protein solution was performed following above procedure and protein activity was calculated using formula (1).

The recombinant protein samples were further analyzed via Coomassie blue SDS-PAGE gels. Protein concentration was measured by Bradford method.

2.4 Preparation of the new biological organic metal material

304 stainless steels (1 mm thick) were annealed at 1040ºC for 1 h, then cut into 1 cm × 1 cm coupons[7]. The surface was polished using sand paper of increasing grit size, from $120^{\#}$-$1200^{\#}$ on the automatic metallographic grinding and polishing machine. Coupons were washed with detergent, then rinsed with distilled water, and immersed in 95% (v/v) alcoholic solution for 15 min. Coupons were then rinsed with distilled water, immersed in acetone for 1 min, and rinsed with distilled water. Coupons were placed into 6 well cell culture plate (1 coupon per well), covered with 3 ml sterile phosphate buffered saline (PBS) (pH7.4）containing a range of concentrations of the recombinant protein, which the final protein concentration were 0.2 μg/μl and 0.4 μg/μl. Then they were incubated at room temperature (RT) for 1 h with gentle agitation. After the reaction, coupons were washed 6 times with distilled water and dried in the air. The reacted sample was denoted as PRM-steel.

2.5 Analysis of the biological organic metal material

To ensure whether the recombinant peptides reacted with the surface of 304 stainless steels, Fourier transform infrared spectroscopy (FTIR) was used to detect the functional groups on PRM-steel samples in compassion to untreated steel samples with an attenuated total reflection (ATR) model of the VERTEX80V FTIR made by Bruker.

X-ray Photoelectron Spectroscopy (XPS) (AXIS-ULTRADLD-600W, Shimadzu-Kratos, Japan) was used to examine the surface electron activity of PRM-steel in comparison to non-treated 304 stainless steel. The base pressure in the analytical chamber was lower than 7×10^{-8} Pa. Monochromatic Al Kα source was used at a power of 450W. The analyses spot was 300×700 μm. The resolution of the instrument was 0.48 eV for Ag 3d 5/2 peak. The scan step was 0.05 eV. XPS spectra were generated by XPS software equipped within the instrument.

The surface morphology samples were examined by a S-4800 scanning electron microscope (SEM) made by Hitachi, Ltd. (Japan HQ). The surface elemental analysis was determined by energy dispersive spectrometer (EDS). The primary electron beam voltage was 10 kV, and the probing beam current was 7 nA.

The contact angles of the samples were tested by the contact angle measuring instrument OCA35 (Dataphysics instruments GmbH). Wettability refers to the degree of affinity of the solid surface and the liquid, measured by the contact angle of a droplet on a solid surface. The droplet used in this study was 1 μl distilled water.

In each test set, at least three parallel groups were used to rule out the randomness of the experiment.

2.6 Statistics

All quantitative measurements were conducted by at least three samples per group and data were expressed as means ± SEM. Groups were compared using independent T-tests. $P \leq 0.05$ was considered statistically significant. *$p \leq 0.05$.

3 Results and discussion

3.1 Vector design

To determine whether the vector design was correct, the screening PCR and gene sequencing were carried out. Screening PCR was conducted by using primers PAF and mal R1 for RPM. The size of amplification fragment was around 1500bp in theory. Clearly, the molecular weight of amplification fragment showed in agarose gel electrophoresis is around 1500bp and matched with the theoretical molecular weight in Fig.2, implying that the vector design was correct. Gene sequencing were used to further determine that the vector sequence was correct or not. The recombinant cells were sequenced by Shanghai Biological Engineering Co., Ltd. The results of sequencing and comparison were shown in Fig.3. Gene sequencing result was in accordance with the basic theory of design sequence. Screening PCR by using primers PhoA F2 and PAR for PRM and subsequent inspections showed the same structure. The size of amplification fragment was around 600bp in theory. Clearly, the molecular weight of amplification fragment showed in agarose gel electrophoresis is around 600bp and matched with the theoretical molecular weight in Fig.4. The results of sequencing and comparison shown in Fig.5 demonstrated a high similarity. The above tests proved that the sequences of two vectors were constructed correctly.

Fig.2 Agarose gel electrophoresis results of screening PCR products of RPM. The band in column 1 indicated by the arrow was the target product, showing the size of the RPM was around 1500bp.

Fig.4 Agarose gel electrophoresis results of screening PCR products of PRM. The band indicated by an arrow was the target product, showing the size of PRM was around 600bp.

Fig.3 The results of gene sequencing and comparison of RPM. Target line is the sequence in theory and sequencing line is the test sequence. The tested gene sequencing results were in accordance with the designed sequences.

Fig.5 The results of gene sequencing of PRM. Target line was the sequence in theory and sequencing line was the test sequence. Gene sequencing results were in accordance with the designed sequence.

3.2 The expression of the recombinant peptide

In order to observe the growth of *E. coli* and the influence of IPTG on the growth rate, the bacterial growth curves were measured. Figures 6 and 7 showed that bacterial grew steadily and IPTG suppressed the proliferation considerably after it was added.
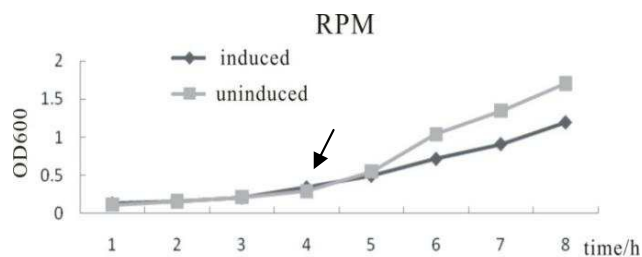
Fig.6 The growth curve of *E.* coli containing plasmid RPM. At 4 hour, IPTG was added (indicated by the arrow) and bacterial growth was restrained.

5
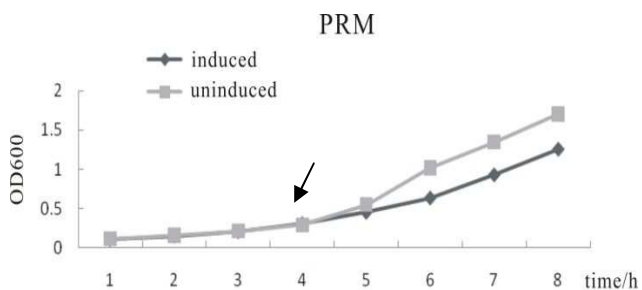
Fig.7 The growth curve of *E.* coli containing plasmid PRM. At 4 hour, IPTG was added (indicated by the arrow) and bacterial growth was restrained.

3.3 Extraction and characterization of the recombinant

10 **protein and its analysis**

Enzymatic activity of PhoA was assayed in whole cells permeabilized by chloroform/SDS and peptide solution treated by Tris-HCl (Fig.8) respectively. It was found that the enzymatic activity of IPTG-induced *E. coli* cells containing PRM was

15 higher than the uninduced *E. coli* cells. However, the enzymatic activity of IPTG-induced *E. coli* cells containing RPM was same with uninduced *E. coli* cells and they didn't have the enzymatic activity of PhoA. In addition, the enzymatic activity of peptide solution of PRM was higher than the *E. coli* cell. These indicated

20 that the RPM did not express the protein whilst the PRM did successfully. Since PhoA only had the enzymatic activity when it was expressed in the periplasm space, and did not show activity when located inside the cell, the cell enzymatic activity of PhoA can be used to detect whether the recombinant protein expressed

25 in the periplasm space. Equally, if the extracted protein solutions had enzymatic activity of PhoA, it indicated that the protein solutions contained the recombinant protein.

Over-expressed recombinant proteins were confirmed via SDS PAGE analysis of total proteins from the cells and the extracted

30 protein solutions (Fig.9). The theoretical molecular weight of mature recombinant protein is about 57 kDa. Clearly, there was not band of RPM in the corresponding position (Fig.9A). However, the molecular weight of recombinant protein PRM shown in SDS PAGE gel matched with the theoretical molecular

35 weight (Fig.9B). These further evidences showed that the recombinant protein RPM could not express and the recombinant protein PRM could express successfully. As a result, the

recombinant protein PRM was used to reaction and analysis in the subsequent experiments.

40
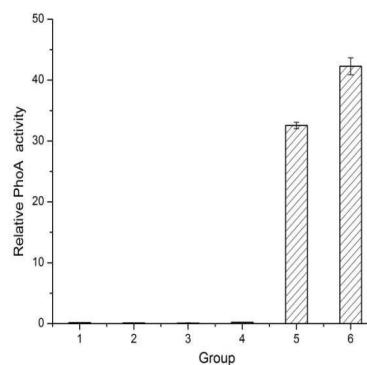
Fig.8 Enzymatic activity of the recombinant protein. 1-3 were the enzymatic activity of the RPM, and 4-6 were the enzymatic activity of the PRM. 1 and 4 were uninduced whole cells; 2 and 5 were the induced whole cells; 3 and 6 were the extracted protein
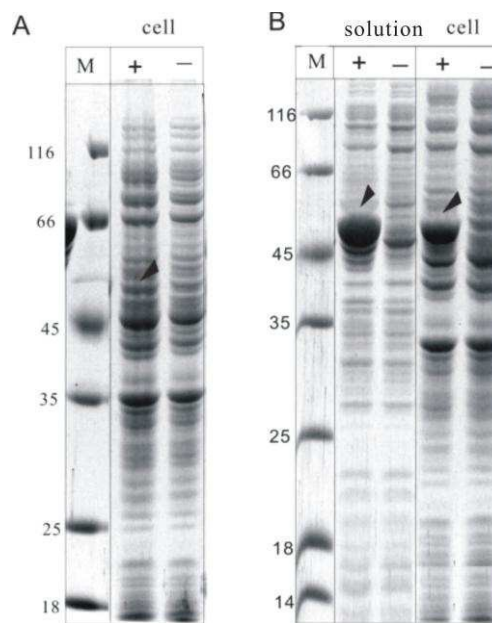
45 solutions.

Fig.9 SDS–PAGE analysis of IPTG-induced (+) or uninduced (-) cells harboring recombinant expression protein and the extracted protein in solutions. A) The SDS-PAGE analysis of whole cell

50 protein harboring RPM vector; B) The SDS-PAGE analysis of extracted PRM protein solution and whole cell protein harboring PRM vector. The arrow heads indicated the targeted protein.

By testing and calculation based on Bradford method, the yield of the fusion protein of all culturing bacteria was between 11.9%

55 and 16.8%.

3.3 Properties analysis of biological organic metal material

After the recombinant protein PRM reacted with 304 stainless steel, the changed properties of the new bioorganic steel, PRM-steel, were examined including the surface chemistry, contact angle, and topography, as a result of the peptide binding.

5 Fourier transform infrared spectroscopy (FTIR) was used to identify new functional groups (Fig.10). Comparing to the untreated 304 stainless steel (Fig.10A) with the PRM-steel (Fig. 10B), multiple new peaks appeared on the spectra. A small peak occurred around the $3100cm^{-1}$, which may be the NH- stretching;

10 the peak around $1650cm^{-1}$ corresponded to C=O stretching; the peak near $1550cm^{-1}$ corresponded to the C-N stretching or NH bending; the peak appearing near $3000cm^{-1}$ corresponded to CH saturated or unsaturated bond[14]. To sum up, the peptide associated bonds (-CO-NH-) have been detected in the surface of

15 the PRM-steel in comparison to the untreated 304 stainless steel. The presence of amide bonds is the characteristic functional groups of the peptide, and they did not exist in untreated 304 stainless steel. Compared the PRM-steel (Fig.10B) with the recombinant peptide solution (Fig.10C), the same peaks with

20 slightly different intensity and the peak shifting were observed (Table 2). Fig.10D showed the combined spectra of A, B, and C to make better comparison. This phenomenon may be caused by the chemical reaction between the recombinant peptides and 304 stainless steel. The chemical reaction caused the small change of

25 functional groups, which ensured that the recombinant peptide can react with stainless steel and firmly combined on the 304 stainless steel through chemical reaction.

30
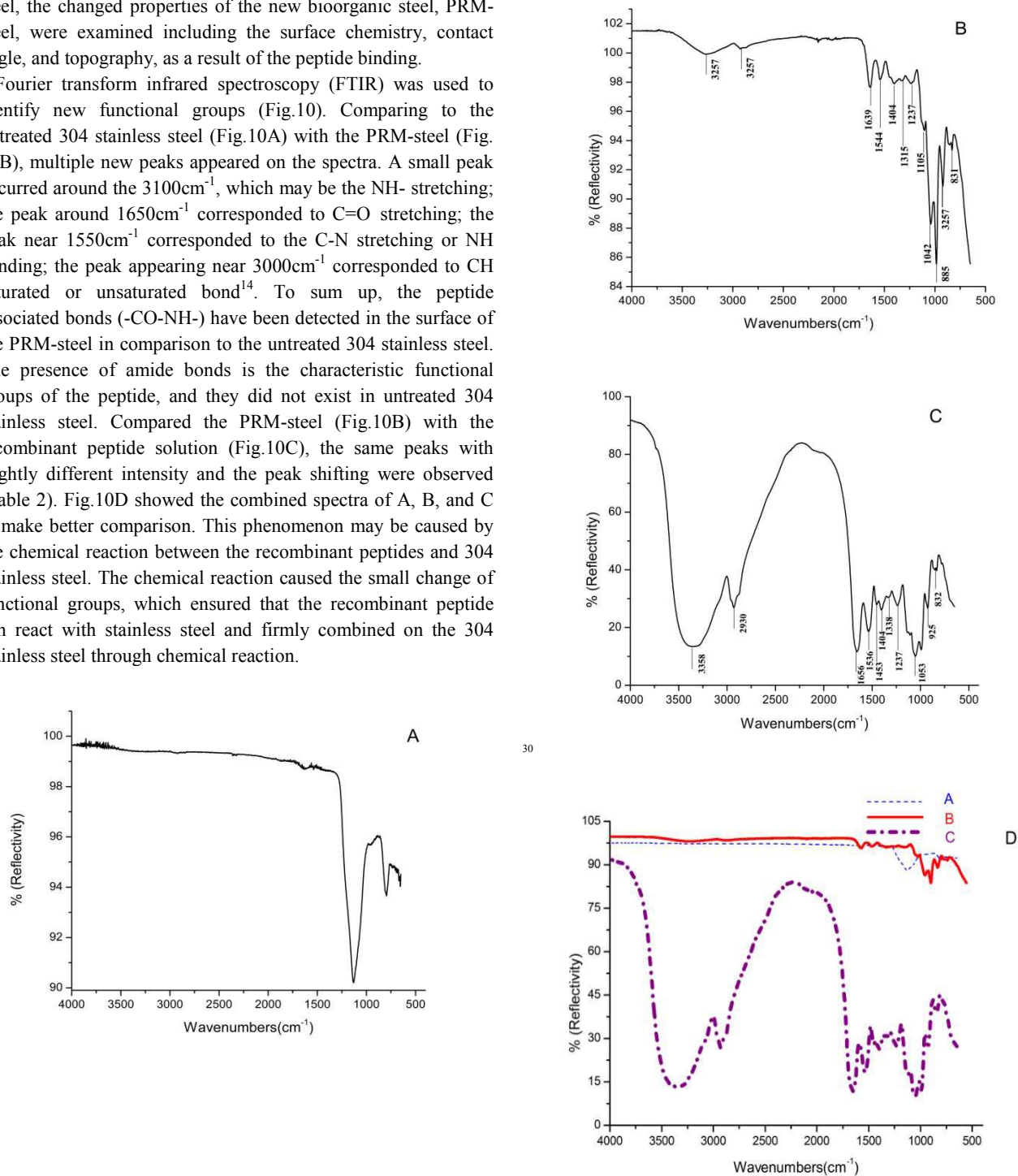
Fig.10 Fourier transform infrared spectra of the samples. A) Untreated 304 stainless steel; B) The PRM-steel; C) The recombinant peptide in solution; D) The combined spectra.

35 In practice, the amide I band in FTIR are primarily used to assign secondary structures to proteins. The IR frequencies in the amide I region, diagnostic of protein secondary structures, are reported in Fig.11. In the image, the peptide FTIR of the PRM-steel were detected peak around the $1643cm^{-1}$. The intense peak

around 1643cm^{-1} was assigned to the Random coil (RC), which demonstrated that the recombinant peptides adsorbing on the steel surface have the stronger secondary structure. Interestedly, the shape of amid I peak was sensitive to the amount of peptide on the metal surface (Fig.11).
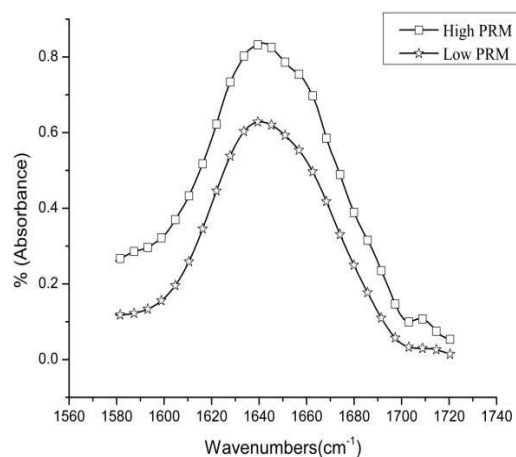
Fig.11 The FTIR spectra of the recombinant peptide absorbing on the 304 stainless steel in the amide I region. The line with square symbol corresponded to the PRM-steel samples reacting with 0.4μg/μl PRM solution. The line with triangle symbol corresponded to the PRM-steel samples reacting with 0.2μg/μl PRM solution.

Table 2 The comparison of the peak values between PRM-steel and PRM protein solution.

Sample	PRM-steel	PRM solution
N-H stretching	3257cm^{-1}	3
C-N stretching	2927cm^{-1}	2930cm^{-1}
C=O stretching	1639cm^{-1}	1656cm^{-1}

Those further proved that the fusion peptide was chemically reacting with the 304 stainless steel by a previously unreported chemical interaction. Such an interaction that generates a new material would result in changes in the electronic state of the surface. To further characterize the chemical properties of PRM-steel, as well as to detect whether new bonding occurred and to identify which elements were involved in the interaction, X-ray photoelectron spectroscopy (XPS) analysis was used to examine the electronic state of the elements on the surface of PRM-steel in comparison to 304 stainless steel. Spectra analysis of the iron, oxygen, sulfur, carbon and nitrogen demonstrated that the iron 2p 1/2 and 2p 3/2 orbitals did not appear to play an important role in bond formation and electron stabilization as no shifts were observed in the PRM-steel when compared to 304 stainless steel (Fig.12A). An increase in the peak of the nitrogen 1S orbital of PRM-steel was observed compared to 304 stainless steel (Fig. 12B), with the PRM-steel N1S peaking at 8500 counts per second (CPS) compared to 3800 CPS for 304 stainless steel, suggesting a role for nitrogen in bond formation. Similarly, an increase in the peak of the carbon 1S orbital of PRM-steel was observed

compared to 304 stainless steel (Fig.12C), with the PRM-steel C1S peaking at 17000 counts per second (CPS) compared to 12000 CPS for 304 stainless steel, suggesting a role for carbon in bond formation. Simultaneously, electron shifts were found in the nitrogen 1S orbital and carbon 1S orbital of PRM-steel compared to 304 stainless steel (Fig.12B and Fig.12C). As a result, nitrogen and carbon play an important role in the formation of the bonds. No significant changes were observed in the spectra of the oxygen 1S and sulfur 2p 3/2 (Fig.12D and Fig.12E). The differences between the electronic states of nitrogen and carbon on the surface of PRM-steel and 304 stainless steel confirmed that PRM-steel was a new material that was chemically different from 304 stainless steel. The XPS spectra data supported the involvement of several elements in the formation of PRM-steel.
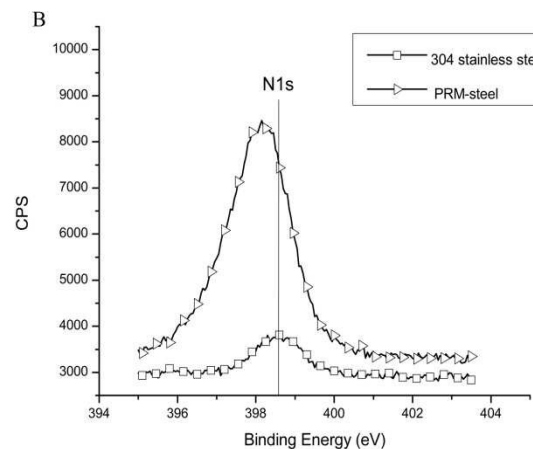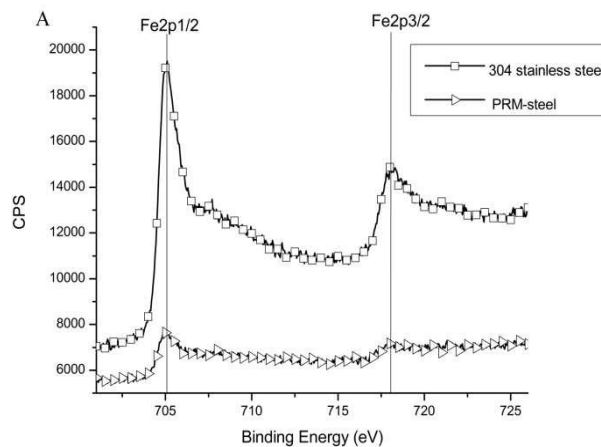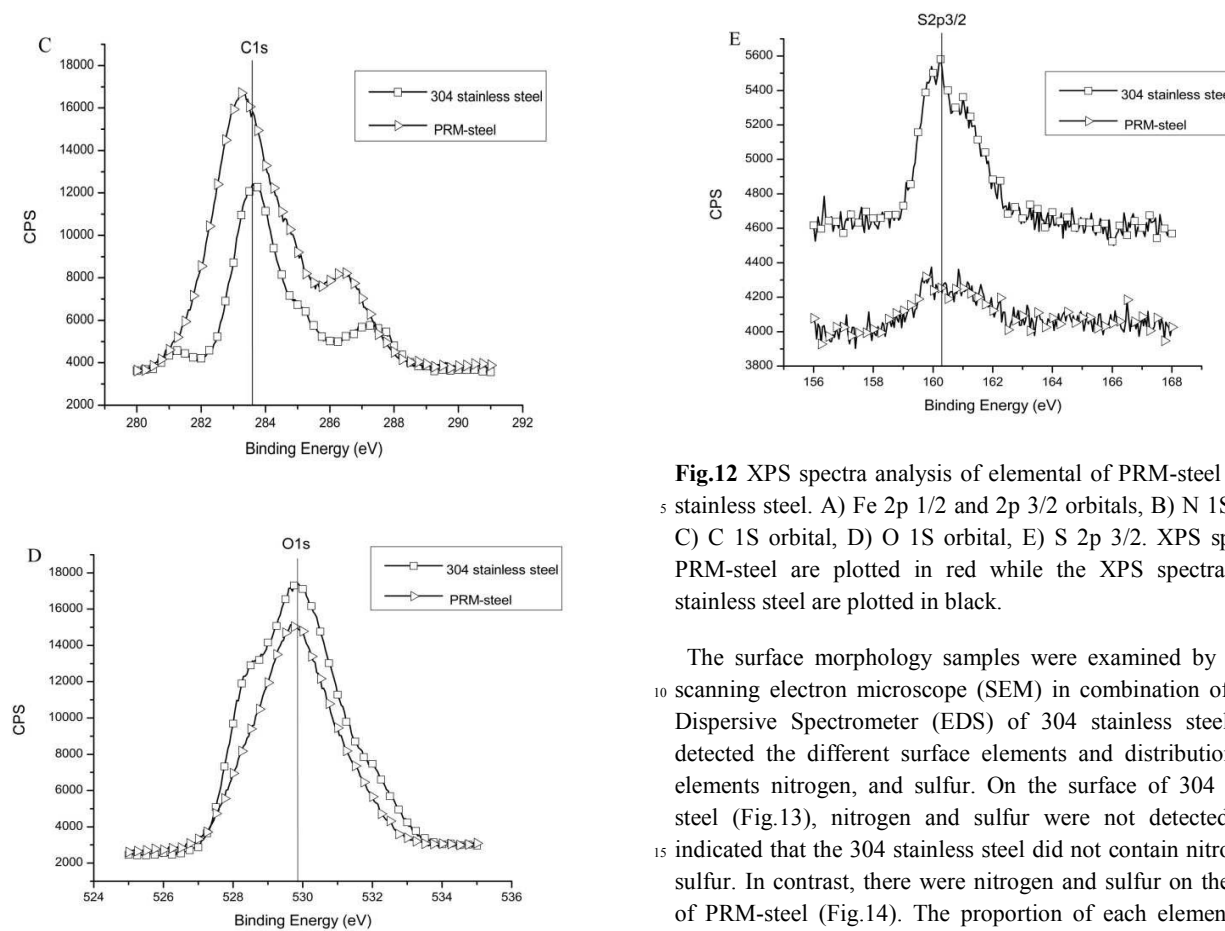
Fig.12 XPS spectra analysis of elemental of PRM-steel and 304 stainless steel. A) Fe 2p 1/2 and 2p 3/2 orbitals, B) N 1S orbital, C) C 1S orbital, D) O 1S orbital, E) S 2p 3/2. XPS spectra of PRM-steel are plotted in red while the XPS spectra of 304 stainless steel are plotted in black.

The surface morphology samples were examined by standard scanning electron microscope (SEM) in combination of Energy Dispersive Spectrometer (EDS) of 304 stainless steel, which detected the different surface elements and distribution of the elements nitrogen, and sulfur. On the surface of 304 stainless steel (Fig.13), nitrogen and sulfur were not detected, which indicated that the 304 stainless steel did not contain nitrogen and sulfur. In contrast, there were nitrogen and sulfur on the surface of PRM-steel (Fig.14). The proportion of each element on the PRM-steel testified that the nitrogen and sulfur element exist on the PRM-steel surface (Fig.14B). The presence of nitrogen and sulfur in PRM-steel surface, which are not normally components of steel surfaces, and the even distribution across the surface on the new PRM-steel surface (Fig.14C and Fig.14D) suggested that the recombinant protein PRM reacted with 304 stainless steel chemically, and the reaction was non-physical adsorption.
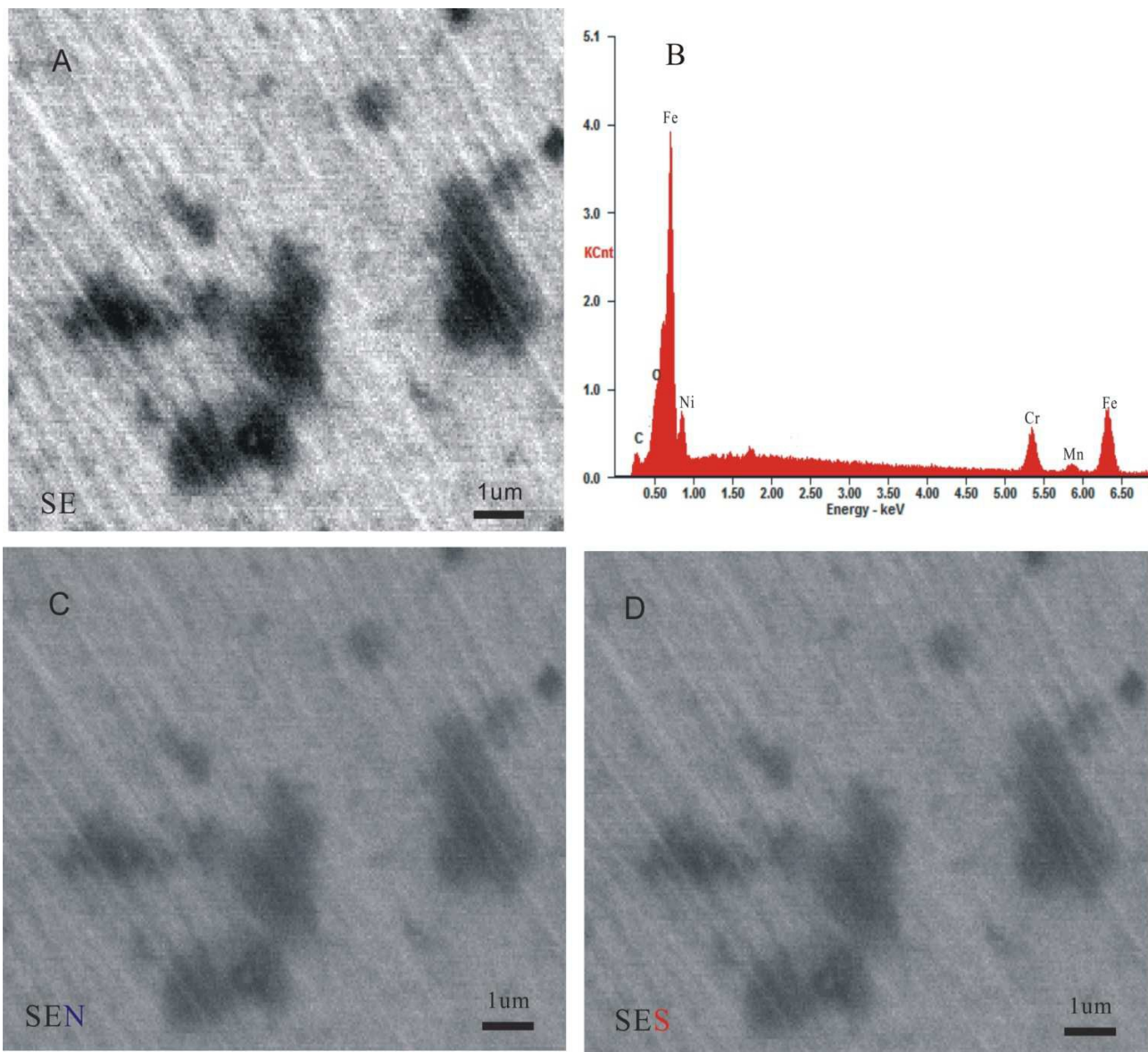
Fig.13 The surface morphology and the distribution of the elements, nitrogen and sulfur, of the original 304 stainless steel. A) Topographical scan of the surface. B) The overall elemental analysis of element on the surface. C) Element scan of nitrogen. D) Element scan of sulfur.
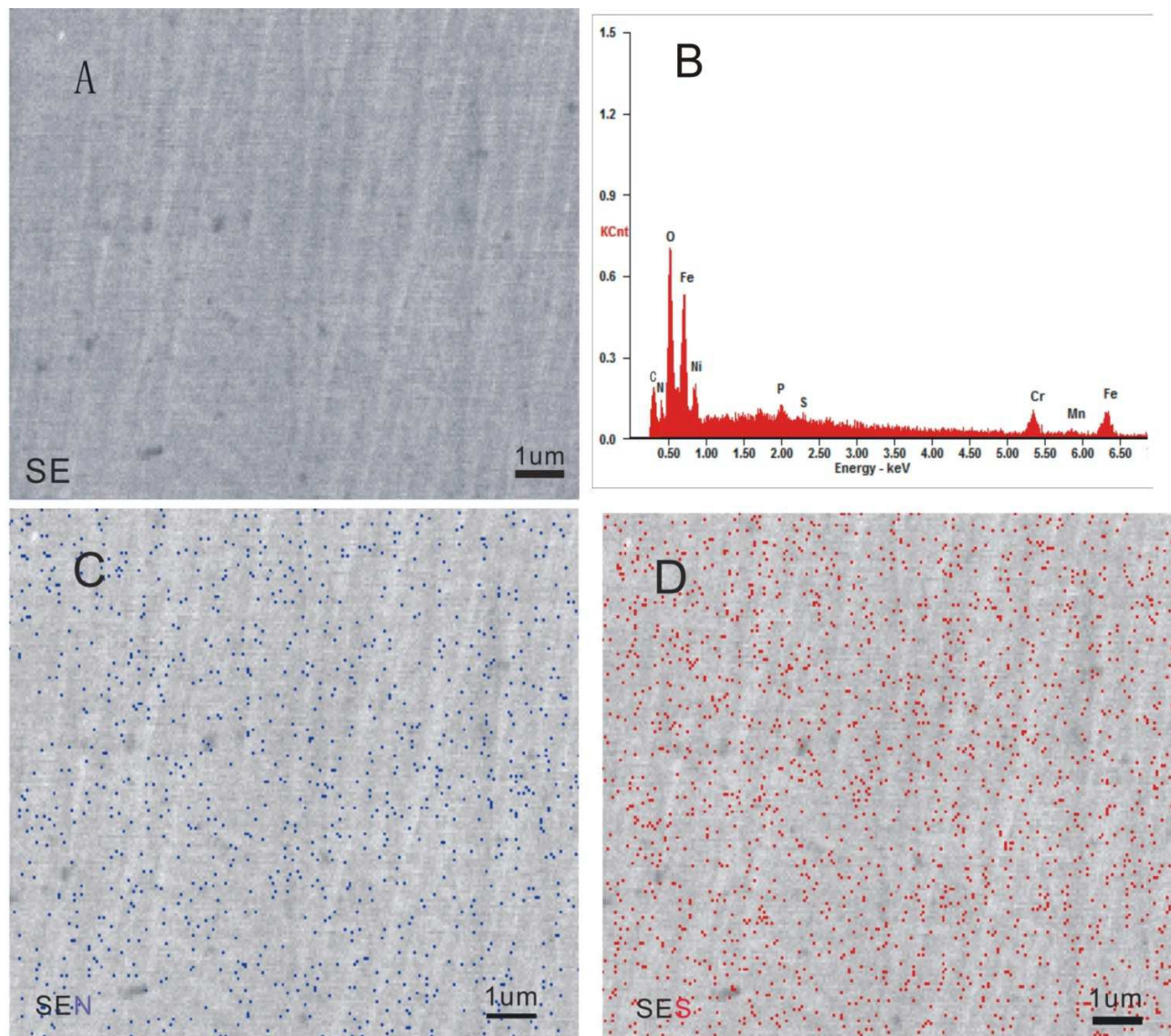
Fig.14 The surface morphology and distribution of the elements nitrogen and sulfur of the new bioorganic material, PRM-steel. A) Topographical scan of the surface. B) The overall elemental analysis of element on the surface. C) Element scan of nitrogen. D) Element scan of sulfur.

5

10

15

The water wettability of the treated and untreated metal surfaces has been tested by the OCA35 automatic contact angle measuring instrument. The greater surface free energy was easier to be infiltrated by some substances, and vice versa. Contact angle is used to measure the spreading capacity between the material surface and the liquid. Generally, the bigger contact angle presents that the affinity between the surface and the liquid is weak[15]. In this report, the contact angle of the new bioorganic steel became bigger than that of the original 304 stainless steel. Moreover, the concentration of recombinant protein participating in the reaction made an influence for the contact angle increase. The higher protein concentration in the reaction, the higher contact angle of bioorganic metal surface changes was resulted (Fig.15).
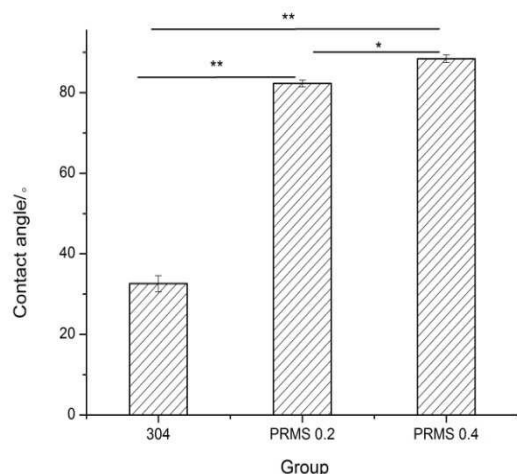
Fig.15 The contact angle of the new bioorganic steel and the regular 304 stainless steel. 304 is the sample of the original 304 stainless steel. The PRMS0.2 is the PRM-steel samples reacting with 0.2µg/µl fusion protein solution. The PRMS0.4 is the PRM-steel samples reacting with 0.4µg/µl fusion protein solution. **P<0.001, 0.001<*P<0.05.

4. Conclusions

We confirm that a smart fusion protein which has metal affinity and hydrophobicity was constructed successfully. Reaction of this new fusion protein with stainless steel at mild reaction condition resulted in a new material, PRM-steel. The multiple assays reveal that the new protein was readily and spontaneously reacted stainless steel, perhaps through the functional adhesion component in the T4P. The PRM-steel has significantly different properties compared with regular 304 stainless steel. The contact angles of the steel were higher than 304 stainless steel, increasing about 50ºC. Moreover, the concentration of recombinant protein participating in the reaction made an influence for the contact angle increase. The higher protein concentration in the reaction, the higher contact angle of bioorganic metal surface changes was resulted. The FT-IR indicated that the characteristic functional group of amide groups on PRM-steel with shifted peak positions compared with the recombinant peptide, which supported that the recombinant peptide had a chemical interaction with 304 stainless steel. The XPS spectra data of PRM-steel revealed that nitrogen element increased and electron state altered, which further indicated that the fusion protein reacted with 304 stainless steel chemically. All of these facts confirmed that the new bioorganic material generated..

The technique that the recombinant peptide bonds with 304 stainless steel to form a new material with altered attributes offered a new method to modify the 304 stainless steel enabling increased contact angle. The optimization of constructed recombinant protein can further increase the contact angle, which could eventually change metal into hydrophobic surface. Importantly such alteration of the metal surface is through an environmental friendly technique, which may support green antifouling.

References

a School of Energy and Power Engineering, Wuhan University of Technology, Wuhan 430063, P.R. China. E-mail: ycq@whut.edu.cn

b School of Medicine, Keele University, Keele, Staffordshire ST5 5BG, United Kingdom

c School of Chemistry, Chemical and Life Sciences, Wuhan University of Technology, Wuhan 430070, P.R. China

d Institute of Biochemistry, Chambroad Chemical Industry Research Institute Co., Ltd, Binzhou 256500, P.R. China

1. L. D. Chambers, K. R. Stokes, F. C. Walsh and R. J. K. Wood, Surface & Coatings Technology, 2006, 201, 3642.
2. A. S. Clare, D. Rittschof, D. J. Gerhart and J. S. Maki, Invertebrate Reproduetion and Development, 1992, 22, 67.
3. D. X. Duan, Marine science, 2011, 35, 107.
4. P. -Y. Qian, S. C. K. Lau, H. -U. Dahms, S. Dobretsov and T. Harder, Marine biotechnology, 2007, 9, 399.
5. H. H. P. Fang, L. C. Xu and K. Y. Chan, Water Research 2002, 36, 4709.
6. Clare A S. Towards nontoxic antifouling, 1998,6,3.
7. E. M. Davis, D. Li and R. T. Irvin, Biomaterials, 2011, 32, 5311.
8. T. H. Swartz, S. Ikewada, O. Ishikawa, M. Ito and T. A. Krulwich, Extremophiles, 2005. 9, 345.
9. C. Yang, H. Xie, J. K. Zhang and B. L. Sun, Protein Expres Purif, 2012, 85, 60.
10. J. E. Coleman, P. Gettins, Advances in Enzymolgy Related Areas of Molecular Biology, 1983, 55: 381.
11. D. Drew, D. Sjöstrand, J. Nilsson, T. Urbig, C. N. Chin, J. W. de Gier and G. von Heijne, Proceedings of the National Academy of Sciences, 2002, 99, 2690.
12. M. H. Malamy and B. L. Horecker, Biochemistry, 1964, 3, 1889.

13.   S. Michaelis, H. Inouye, D. Oliver and J. Beckwith, Journal
      of Bacteriology, 1983, 154, 366.
14.   M. Carbonaro and A. Nucara, Amino acids, 2010, 38, 679.
15.   X. J. Fan, Dalian University of Technology, 2012.